This is the peer reviewed version of the following article: [Pharmacol Res. 2019 Jul;145:104260], which has been published in the final form at doi: 10.1016/j.phrs.2019.104260. This article may be used for noncommercial purposes in accordance with Elsevier terms and conditions for use of self-archived version

Pharmacological Research xxx (xxxx) xxx-xxx

Contents lists available at ScienceDirect

Pharmacological Research

journal homepage: www.elsevier.com

Proof-of-concept validation of the mechanism of action of Src tyrosine kinase inhibitors in dystrophic *mdx* mouse muscle: *in vivo* and *in vitro* studies

F. Sanarica [a], P. Mantuano [a], E. Conte [a], A. Cozzoli [a], R.F. Capogrosso [a, b], A. Giustino [c], A. Cutrignelli [a], O. Cappellari [e], J.F. Rolland [d], M. De Bellis [a], N. Denora [a], G.M. Camerino [a], A. De Luca [a, *]

[a] *Department of Pharmacy - Drug Sciences, University of Bari "Aldo Moro", 70121 Bari, Italy*
[b] *Department of Chemical, Toxicological and Pharmacological Drug Studies, Catholic University "Our Lady of Good Counsel", Tirana, Albania*
[c] *Department of Biomedical Sciences and Human Oncology, School of Medicine, University of Bari "Aldo Moro", 70121, Bari, Italy*
[d] *AXXAM S.p.A., Openzone, 20091, Bresso, Milan, Italy*
[e] *Division of Cell Matrix Biology and Regenerative Medicine, University of Manchester, Manchester Academic Health Science Centre, UK*

ARTICLE INFO

Keywords:
Duchenne muscular dystrophy
Preclinical study
mdx mouse model
Src tyrosine kinase inhibitors
Oxidative stress

ABSTRACT

Src tyrosine kinase (TK), a redox-sensitive protein overexpressed in dystrophin-deficient muscles, can contribute to damaging signaling by phosphorylation and degradation of β-dystroglycan (β-DG). We performed a proof-of-concept preclinical study to validate this hypothesis and the benefit-safety ratio of a pharmacological inhibition of Src-TK in Duchenne muscular dystrophy (DMD).

Src-TK inhibitors PP2 and dasatinib were administered for 5 weeks to treadmill-exercised *mdx* mice. The outcome was evaluated *in vivo* and *ex vivo* on functional, histological and biochemical disease-related parameters. Considering the importance to maintain a proper myogenic program, the potential cytotoxic effects of both compounds, as well as their cytoprotection against oxidative stress-induced damage, was also assessed in C2C12 cells.

In line with the hypothesis, both compounds restored the level of β-DG and reduced its phosphorylated form without changing basal expression of genes of interest, corroborating a mechanism at post-translational level. The histological profile of gastrocnemius muscle was slightly improved as well as the level of plasma biomarkers. However, amelioration of *in vivo* and *ex vivo* functional parameters was modest, with PP2 being more effective than dasatinib. Both compounds reached appreciable levels in skeletal muscle and liver, supporting proper animal exposure. Dasatinib exerted a greater concentration-dependent cytotoxic effect on C2C12 cells than the more selective PP2, while being less protective against H_2O_2 cytotoxicity, even though at concentrations higher than those experienced during *in vivo* treatments.

Our results support the interest of Src-TK as drug target in dystrophinopathies, although further studies are necessary to assess the therapeutic potential of inhibitors in DMD.

Abbreviations: Ab, antibody; Ag, antigen; AMPK, AMP-activated protein kinase; Bnip3, BCL2/adenovirus E1B 19 kDa protein-interacting protein 3; BW, body weight; CCK-8, Cell Counting Kit-8; CK, creatine kinase; CNF, centronucleated fibres; CNRF, centronucleated regenerating fibres; DGC, dystrophin-glycoprotein complex; DMD, Duchenne muscular dystrophy; DMSO, dimethyl sulfoxide; EDL, extensor digitorum longus; ELISA, enzyme-linked immunosorbent assay; ERK1/2, extracellular signal regulated kinase 1/2; GADPH, glyceraldehyde-3-phosphate dehydrogenase; GC, gastrocnemius; H&E, hematoxylin-eosin; HPLC, high performance liquid chromatography, i.p.: intraperitoneal injection; LDH, lactate dehydrogenase; MMP-9, matrix metalloproteinase-9; NF, normal myocyte; NOX, NADPH oxidase; PBS, phosphate buffer saline; PDN, α-methyl-prednisolone; PGC-1α, proliferator-activated receptor γ coactivator-1; PK, pharmacokinetic; PP2, 4-Amino-3-(4-chlorophenyl)-1-(t-butyl)-1H-pyrazolo[3,4-d] pyrimidine, 4-Amino-5-(4-chlorophenyl)-7-(t-butyl) pyrazolo[3,4-d] pyrimidine; p-βDG, phospho-β-dystroglycan; ROS, radical oxygen species; s.c., subcutaneous; SEM, standard error of the means; sP0, maximal isometric tetanic tension; sPtw, maximal isometric twitch tension; TA, tibialis anterior; TGF-β1, transforming growth factor beta 1; TK, tyrosine kinase; Utrn, utrophin; WT, wild type; β-ACT, β-actin; β-DG, β-dystroglycan.

* Corresponding author at: Unit of Pharmacology, Department of Pharmacy - Drug Sciences, University of Bari, "Aldo Moro", Orabona 4, Campus, 70121, Bari, Italy.
Email address: annamaria.deluca@uniba.it (A. De Luca)

https://doi.org/10.1016/j.phrs.2019.104260
Received 13 January 2019; Received in revised form 8 April 2019; Accepted 1 May 2019
Available online xxx
1043-6618/ © 2019.

UNCORRECTED PROOF

1. Introduction

Duchenne muscular dystrophy (DMD, #310200) is a rare disease characterized by significant disability, progressive functional impairment and muscle wasting. Mutations in the dystrophin gene characterize the pathology, leading to severe DMD in humans and to dystrophic conditions in animals such as the *mdx* mouse model, widely used for preclinical studies [1]. Nowadays, glucocorticoids are the sole drugs able to delay pathology progression and control symptoms in DMD boys [2], even though significant progresses have been made in enhancing dystrophin expression by correcting or replacing the defective gene [3,4]. Some of these strategies are under evaluation at clinical stage, even though these approaches have limited efficacy and are often mutation-specific, therefore they address a limited percentage of patients [5]. An intense research is ongoing to identify small molecules, potentially helpful for all DMD boys, that contrast disease progression by targeting pathology-related events downstream the main defect, with less side effects with respect to clinically used steroids. The absence of dystrophin and the consequent disassembling of the dystrophin-glycoprotein complex (DGC) cause progressive muscle degeneration and aberrant signaling during contraction. A first consequence of dystrophin absence is the disorganization of the DGC with reduction of β-dystroglycan (β-DG), a protein involved in the signal transduction process that ensures adequate metabolic response to contractile stress [6,7]. In fact, it is known that β-DG interacts with AMP-activated protein kinase (AMPK), a key regulator of energy metabolism that acts as a sensor of cellular energy levels and its absence may contribute to defective activation of this pathway by exercise and drugs [8,9]. In absence of dystrophin, a critical Tyrosine (Tyr892) residue of β-DG is exposed and phosphorylated by a member of Src tyrosine kinase (TK) family, leading to its internalization and degradation by proteasome [10]. Recently, we have shown that Src-TK is overexpressed in dystrophin-deficient muscles and can be overactive due to excessive radical oxygen species (ROS) production [11–13], since NADPH oxidase (NOX)-related oxidative stress is a primary pathological event in dystrophic myofibers, being detectable before pathology onset [11,14,15]. These damaging pathways are exacerbated by a chronic exercise protocol, and we demonstrated a faulty adaptive mechanism of dystrophic muscles to chronic exercise by means of both proteomic and genomic studies, with a drastic alteration of key anti-oxidant metabolic pathways and contractile proteins and increase of several glycolytic enzymes and fast twitch fibre proteins [12,16].

Importantly, Src-TKs are activated by ROS *via* thiol oxidation and play a critical role in ROS-mediated cellular signaling such as cell survival and growth, metabolism, inflammation, autophagy and, in turn, reinforcing oxidative stress by phosphorylation and activation of NOX [11,17,18]. Previous studies from Winder's group have suggested that in *mdx* mice, the reduction of Tyr phosphorylation , obtained by crossing it with a knock-in mouse having a Phenylalanine replacing Tyr892, restores β-DG and other DGC proteins, with an amelioration of dystropathology [19]. In addition, a similar rescue of β-DG and DGC components has been observed in both *mdx* mice that lack dystrophin and in muscle explants from DMD patients after inhibition of the proteasome [20,21]. Taken together, these data reinforce the interest in inhibiting Src-TK by small drugs to reduce β-DG phosphorylation, with the consequent restoration of DGC complex. Furthermore, impaired autophagy, reported in dystrophic muscle, may underlie muscle degeneration [22] and recent evidence show that activated Src-TK leads to a block of this evolutionary conserved cellular degradation pathway in *mdx* skeletal muscle; thus, the inhibition of Src-TK partially rescues the defective autophagy in dystrophic myofibers [11].

Considering this evidence, our working hypothesis is that the inhibition of Src-TK can beneficially target the pathogenetic cascade leading to muscle wasting in DMD acting both downstream, by counteracting oxidative stress, inflammation and autophagy, and upstream, by reducing the phosphorylation and degradation of β-DG. In particular, we focused on two small molecules acting as Src-TK inhibitors: the highly selective 4-Amino-3-(4-chlorophenyl)-1-(t-butyl)-1H-pyrazolo[3,4-d] pyrimidine, 4-Amino-5-(4-chlorophenyl)-7-(t-butyl) pyrazolo[3,4-d] pyrimidine (PP2) and the anticancer drug dasatinib, already in clinical use for the treatment of chronic myeloid leukemia [23]. In particular, PP2, tested *in vitro*, protects *mdx* muscle from contraction-induced weakness and restores autophagy [13]. More recently, it has been demonstrated that dasatinib decreases the levels of β-DG phosphorylation on tyrosine, and increases the relative levels of non-phosphorylated β-DG in *sapje* zebrafish [24]. However, no proof-of-concept in *in vivo* preclinical studies have been performed to assess both efficacy and safety profile of Src-TK inhibitors on the pathophysiology of dystrophic *mdx* mouse model. Thus, we performed a 5-week proof-of-concept study with these two Src-TK inhibitors on chronically exercised *mdx* mice currently in use in our laboratories, for preclinical drug tests [14], either to investigate their potential protective effect on muscle functionality or to assess any potential limitations in their use in muscular dystrophy.

Efficacy and safety of PP2 and dasatinib have been evaluated with a multidisciplinary approach, on a large array of *in vivo* and *ex vivo* readout parameters. Moreover, to gain insight into the mechanism of action of Src-TK inhibitors on dystrophic skeletal muscle and their potential interference with myogenic program, we conducted *in vitro* studies on C2C12 cells, a murine muscle derived satellite cell line. The effects of these two compounds were tested on cell viability and on oxidative stress-induced cytotoxicity. The final aim of this study is to pave the way to the identification and design of novel drugs with clear impact in the treatment of all DMD patients, irrespective to mutation.

2. Materials and methods

All experiments were conducted in conformity with the Italian law for Guidelines for Care and Use of Laboratory Animals (D.L. 116/92), and European Directive (2010/63/UE). The experimental protocol was approved by the Italian Minister of Health (Authorization n. 815/2017-PR). Most of the experimental procedures used respected the standard operating procedures for pre-clinical tests in *mdx* mice available on the TREAT NMD website (http://www.treat-nmd.eu/research/preclinical/dmd-sops/).

2.1. In vivo studies

2.1.1. Experimental groups, exercise protocols and drug treatments

A total of 24 *mdx* male mice (C57/BL10ScSn-Dmd^{mdx}/J), homogeneous for body weight (BW), fore limb force and exercise resistance, were used for this study at an initial age of 4–5 weeks (Charles River, Italy for Jackson Laboratories). The duration of the treatment was chosen to be 5 weeks to minimize the occurrence of potential toxicity, considering that non-receptor Src-TK plays a vital role in many facets of cell physiology [18,23] and the lack of information about Src-TK inhibitors effects in mammalian models for DMD. For the entire duration of the treatment, the mice, either vehicle or drug treated, underwent 30 mins running on a horizontal treadmill (Columbus Instruments, USA) at 12 m/min, twice a week with a consistent 48–72 hours break between each exercise session [25]. The exercise protocol facilitates the estimation of drug efficacy on pathology-related parameters, (http://www.treat-nmd.eu/resources/research-resources/dmd-sops) [25,26]. Thus, the groups were as follows: 8 *mdx* mice vehicle-treated; 8 *mdx* mice treated with 5 mg/kg PP2 (Sigma-Aldrich, Italy) and 8 *mdx* mice treated with 5 mg/kg dasatinib (kindly provided by Bristol-Myers Squibb, BMS, in the frame of a no-profit project n. CA180-613 and then

UNCORRECTED PROOF

purchased by Selleckchem, USA). A group of 6 wild type (WT) mice of same age and gender (WT, C57/BL10ScSn/J), only undergoing cage-based activity (sedentary WT) was also used for specific experimental purposes and monitored at the same time points of *mdx* counterparts. Both PP2 and dasatinib were chosen as candidate compounds for their ability to inhibit Src-TK in the low nanomolar range (IC_{50} = 36 and 0.8 nM, respectively) [27]. The dose of PP2 and dasatinib have been chosen based on available pharmacokinetic and experimental data in mouse [28]. Considering the poor oral bioavailability and their low aqueous solubility, PP2 and dasatinib were dissolved in oil depot formulations (1% dimethyl sulfoxide, DMSO, in corn oil solution; Sigma-Aldrich, Italy) and were administered three times a week by subcutaneous (s.c.) injection. The dose was formulated so to inject 0.1 ml of vehicle/10 g of BW. The treatment started one day before the beginning of the exercise protocol and continued until the day of sacrifice. Care in animal handling and environment conditions was used to avoid any animal discomfort and stress during injection. Food intake was monitored and composition, detailed elsewhere, was maintained constant [29]. Every week, all mice were monitored for BW and forelimb force by means of a grip strength meter (Columbus Instruments, USA). The final time point for *in vivo* parameters was the end of the 5th week of exercise/treatment (T5) and was considered for statistical analysis [26]. At T5, as well as at the beginning of the protocol (time 0, T0) an exercise resistance test on treadmill was also performed. At the end of the 5th week of exercise/treatment, after assessment of *in vivo* endpoints, the *ex vivo* experiments were also started. Due to the time-consuming nature of some of the *ex vivo* procedures, no more than two animals were sacrificed *per* day. This required to prolong the experimental time window of about 2 weeks. Thus, the animals continued to be exercised/treated until the day of sacrifice, but no longer than 7 weeks in total. Importantly, animals of each experimental group were equally distributed over time for the *ex vivo* experiments so to avoid bias due to different exposure to exercise and/or treatment. This approach has been long validated in our laboratory [14,30]. Due to the progressive reduction in the number of animals in each group between the 5th and 7th week, no statistical analysis was performed on BW and grip strength data that were collected in this time window to verify constant animal state over time.

2.1.2. In vivo torque

In vivo maximal isometric torque of the plantarflexor muscle group (gastrocnemius and soleus muscles) was assessed at the various time points of chronic exercise activity as described previously [31]. Mice were anaesthetized *via* inhalation (≃4% isoflurane and 1.5% O_2 l/min) and placed on a thermostatically controlled table; anesthesia was maintained *via* a nose cone (≃2% isoflurane and 1.5% O_2 l/min). The right hind limb was shaved and aseptically prepared and the foot was placed on the pedal connected to a servomotor (model 300C-LR; Aurora Scientific, Aurora, ON, Canada). Contractions were elicited by percutaneous electrical stimulation of the tibial nerve *via* needle electrodes (Chalgren Enterprises) connected to a stimulator (model 701B; Aurora Scientific) to induce contraction of the group of plantar flexor muscles. The current was adjusted from 30 to 50 mA until maximal isometric torque was achieved, and a series of stimulations was then performed at increasing frequencies [31]. Data were analyzed using Dynamic Muscle Analysis software (DMAv5.201; Aurora Scientific) to obtain torque, which was normalized to mouse BW. Normalized values were used to construct torque-frequency curves.

2.2. Ex vivo studies

2.2.1. Muscle preparation

Animals belonging to the different groups were anesthetized with ketamine (100 mg/kg, intraperitoneal injection, i.p.) combined with xylazine (16 mg/kg, i.p.). If necessary, half the dosage of only ketamine was administered to mice to obtain a deep plane of anesthesia. The extensor digitorum longus (EDL) muscle of one hind limb was removed and rapidly placed in the recording chambers for isometric and eccentric contraction measurements. GC muscle from one hind limb was removed, washed in phosphate-buffered saline (PBS) and snap frozen in isopentane, cooled in liquid N_2 and stored at −80 °C until processed for histological analysis. Contralateral gastrocnemius (GC) and tibialis anterior (TA) muscle from one hind limb were snap frozen in liquid N_2 and stored at −80 °C until use for molecular biology studies (qRT-PCR and western blot analysis, respectively). Organs, such as heart, spleen, and kidney were removed and weighed, to assess any possible toxic drug effect.

2.2.2. Protein expression analysis by immunoprecipitation and western blot

Protein extractions and immunoblots for the determination of β-DG and β-actin (β-ACT), detected as reference standard, were performed in TA muscles of different experimental groups. TA muscles from α-methyl prednisolone (PDN)-treated *mdx* mice from previous experimental groups with comparable conditions (exercise, duration of treatment and animal age) were also used as internal positive controls [32]. TA muscles from exercised WT and exercised *mdx* mice were homogenized in ice-cold buffer containing 20 mM Tris-HCl (pH 7.4 at 4 °C), 1% (v/v) Triton X-100, 1% (v/v) NP-40, 2 mM $MgCl_2$, 5 mM EDTA, 150 mM NaCl, 0.2 mM phenylmethylsulfonyl fluoride, 1 mM $NaVO_4$, 10 mM NaF and protease inhibitors (10 mg/ml leupeptin and 10 mg/ml pepstatin). Homogenates were centrifuged at 1000 × g for 10 mins at 4 °C and the supernatant was quantified using Bradford protein assay kit (Bio-Rad Protein Assay Kit I5000001). For the determination of phospho-β-dystroglycan (p-βDG), before immunoblot analysis, immunoprecipitation was performed: 10 μl of mouse primary antibody (Ab) anti-βDG, diluted in 200 μl of PBS-Tween-20, were added to Dynabeads protein G (Life Technologies) and incubated for 3 hours at 4 °C on a roller for mixing. After three washes with PBS, 60 μg of protein extract (antigen, Ag) were added and samples were incubated overnight at 4 °C on a roller for mixing. After three washes with PBS, Dynabeads-Ab-Ag complex was resuspended in 20 μl of Elution Buffer, added with 20 μl premixed NuPage LDS Sample Buffer and NuPage Sample Reducing Agent (Life Technologies), and heated for 10 mins a 70 °C. Protein content was quantified using Bradford protein assay kit (Bio-Rad Protein Assay Kit I5000001). For immunoblot analysis, 60 μg of protein were separated on a 12% SDS-PAGE and transferred onto PVDF membrane for 1 hour at 200 mA (SemiDry transferblot; Bio-Rad), and protein detection was conducted as described previously [31]. The following dilutions of primary antibodies were used: 1:200 mouse anti β-DG (Novocastra); 1:500 mouse anti p-βDG (Abcam) and 1:300 mouse anti β-ACT (Santa Cruz Biotechnologies). An anti-mouse horseradish peroxidase-conjugated secondary antibody (1:5000 anti-mouse IgG, Sigma-Aldrich) was used. β-ACT was detected after stripping membrane with 200 mM glycine, 3.5 mM SDS and 1% Tween-20, pH 2.2. Densitometric analysis was performed using Image Laboratory software (Bio-Rad). The software allows the chemiluminescence detection of each experimental protein band to obtain the absolute signal intensity. The density volume was automatically adjusted by subtracting the local background.

2.2.3. Isolation of total RNA, reverse transcription and real-time PCR

For each GC muscle, total RNA was isolated by RNeasy Fibrous Tissue Mini Kit (cat. no. 74704; Qiagen) and quantified by spectrophotometry (ND-1000 NanoDrop; Thermo Scientific). To perform reverse transcription for each sample was prepared with standard procedure previously described [31,33] and according to SuperScript II Reverse Transcriptase kit instruction (cat. no. 18064014, ThermoFisher). Real-time PCR was performed using the Applied Biosystems Real-time PCR

UNCORRECTED PROOF

7500 Fast system, MicroAmp Fast Optical 96-Well Reaction Plate 0.1 ml (cat. no. 4346906; Life-Technologies) and MicroAmp Optical Adhesive Film (cat. no. 4311971; Life Technologies). Each reaction was carried in duplicate on a single plex reaction. Reactions consisted of 8 ng of cDNA, 0.5 μl of TaqMan Gene Expression Assays, (Life Technologies) and 5 μl of TaqMan Universal PCR master mix No AmpErase UNG (2X) (cat. no. 4324018; Life Technologies) and Nuclease-Free Water not DEPC-Treated (cat. no. AM9930; Life-Technologies) for a final volume of 10 μl. RT-TaqMan-PCR conditions were as follows: step 1: 95 °C for 20 s; step 2: 95 °C for 3 s; and step 3: 60 °C for 30 s; steps 2 and 3 were repeated 40 times. The results were compared with a relative standard curve obtained from five points of 1:4 serial dilutions. The mRNA expression of the genes was normalized to the housekeeping gene glyceraldehyde-3-phosphate dehydrogenase (GADPH). TaqMan hydrolysis primer and probe gene expression assays were ordered with the following assay IDs: GADPH, assay ID: Mm99999915_g1; β-DG, assay ID: Mm00802400_m1; utrophin (Utrn), assay ID: Mm01168866_m1; cSrc-TK, assay ID: Mm00432751_m1; BCL2/adenovirus E1B 19 kDa protein-interacting protein 3 (Bnip3), assay ID: Mm01275600_g1; NOX, assay ID: Mm01287743_m1 and transforming growth factor β 1 (TGF-β1), assay ID: Mm01178820_m1. All gene expression experiments were conducted following the MIQE guideline [34].

2.2.4. Muscle histopathology

GC muscles, previously frozen in liquid N_2-cooled isopentane, were transversally cut on a cryostat and 6–8 μm sections were stained with hematoxylin-eosin (H&E) to calculate the percentage of healthy myofibers with peripheral nuclei (NF), regenerating/regenerated myofibers, showing central nuclei (CNF), as well as the total area of damage (necrosis, inflammation, and non-muscle area). Morphometric analysis was performed by using ImageJ analysis software on the entire muscle section, randomly selecting approximately three fields per section at 10X magnification for muscle damage and six fields per section at 20X magnification for counting centronucleated and peripherally nucleated myofibers. For each muscle, two sequential cross sections were used; at least five animals per experimental group were assessed. The total area of damage was quantified by using ImageJ analysis software. In particular, the percentage of damage was calculated with respect to the total area of the field considered and the mean of at least five fields *per* animal was calculated.

2.2.5. Immunofluorescence analysis

Immunofluorescence analysis was performed on 6–8 μm sections of GC previously cut at the cryostat. Immunofluorescence staining was performed as previously described [32]. The following primary antibodies were used: mouse anti-β-dystroglycan, 1:100 (Novocastra) and rabbit anti-laminin, 1:200 (Sigma-Aldrich). The secondary antibodies used were: Alexa Fluor 488 donkey anti-mouse and Alexa Fluor 546 donkey anti-rabbit (Life Technologies), with 1:500 dilution. Images were then taken with a fluorescence microscope (CX41, Olympus, Rozzano, Italy).

2.2.6. Isometric and eccentric contraction

For contractile recordings, EDL muscle was securely tied at the tendon insertion and placed in a muscle chamber containing a normal physiological Ringer's solution (in mM): 148 NaCl, 4.5 KCl, 2.0 $CaCl_2$, 1.0 $MgCl_2$, 12.0 $NaHCO_3$, 0.44 NaH_2PO_4 and 5.55 glucose, continuously gassed with 95% O_2-5% CO_2 (pH 7.2–7.4) at a constant temperature (27 ± 1 °C). One tendon was fixed to a force transducer (FORT25, WPI or a 1 N 300C-LR, Aurora Scientific) connected to proper interface and acquisition units (TCI 102 interface and an MP 100 acquisition unit, Biopac Systems, Santa Barbara, CA or Dynamic Muscle Control Acquisition System v.5.415; ASI). Electrical field stimulation was obtained by two platinum electrodes connected to a stimulator (LE 12406; 2Biological Instruments) that closely flanked the muscle. After equilibration (30 min.), the preparation was stretched to its optimal length (L0; measured with calipers), *i.e.* the length producing the maximal twitch in response to a 0.2 ms square wave 40 to 60 V pulse. A force frequency relationship was obtained with trains of 350 ms duration over a range of frequencies (10–250 Hz). Eccentric contraction force drop as well as recovery were assessed as described previously [9,31]. An index of stiffness during each eccentric contraction was measured by dividing the difference in force produced between the isometric response and the peak force resulting from the imposed stretch (*i.e.*, change in force) by the change in muscle length during the stretch (0.1 L0) [35].

The same protocol of isometric contraction recordings was performed on contralateral EDL muscles from WT and *mdx* mice, to assess the acute effects of increasing concentrations of dasatinib (10, 50, 100, 150 μM) *in vitro*. These concentrations were chosen based on the results obtained from cytotoxicity *in vitro* assays, described further below in the paper. After a first isometric contraction protocol in normal Ringer's solution, EDL muscles underwent the same recordings for every concentration of dasatinib (dissolved in Ringer's solution), starting from 10 μM up to 150 μM, with an incubation period of 30 mins prior to the beginning of each protocol. In parallel, a control group of EDL muscles from both WT and *mdx* mice undergoing the same protocol, was incubated with the vehicle alone (DMSO 0.15% in Ringer's solution).

2.2.7. Blood samplings and determination of CK, LDH and MMP-9 plasma levels

Blood was obtained from cardiac puncture of the left ventricle with a heparinized syringe and collected in heparinized tubes. Blood were left for 10 mins on ice. Plasma samples were obtained after centrifugation for 20 mins at 2000 × g at 4 °C, then, an additional centrifugation step for 10 mins at 1500 × g at 4 °C was performed for complete platelet removal. Creatine kinase (CK) and lactate dehydrogenase (LDH) were determined on the day of plasma preparation by standard spectrophotometric analysis, using diagnostic kit (Sentinel, Farmalab - Italy). Platelet-poor plasma samples were stored at −20 °C until use for determination of matrix metalloproteinase (MMP-9). MMP-9 was measured in 20-fold diluted plasma samples by enzyme-linked immunosorbent assay (Quantikine ELISA Mouse Total MMP-9 Immunoassay R&D Biosytems ELISA), according to the manufacturer's instructions. The optical density of each well was determined, using a microplate reader set to 450 nm (Victor Victor V31420-40, PerkinElmer, Wellesley, Massachusetts). A standard curve was generated to obtain MMP-9 levels expressed in ng/ml. All the remaining serum was collected and stored at −20 °C for further pharmacokinetic (PK) investigation by High performance liquid chromatography (HPLC) analysis to determine PP2 and dasatinib plasma levels.

2.2.8. Pharmacokinetic analysis by HPLC

For plasma samples the analysis was performed with a 1100 Series liquid chromatograph (Hewlett Pachard) and a 6530 Accurate-mass QTOF LC/MS spectrometer (Agilent Technologies) equipped with an electrospray ion source and controlled by Masshunter Workstation software (Agilent Technologies). Chromatographic separation was achieved on an Agilent Zorbax SB-C18 (3.0 mm × 150 mm, 5 μm) column, with water-0.1% formic acid and acetonitrile as mobile phase. The flow rate was 0.5 mL/min. Drying gas flow and nebulizer pressure were set at 8 l/min and 35 psig. Dry gas temperature and capillary voltage of the system were adjusted at 300 °C and 3500 V, respectively. LC/MS was used to quantification using target fragment ions in positive ion electrospray ionization interface.

For PK analysis in muscle and liver, tissues were individually weighed into a "FastPrep" tube and PBS was added (3:1 ratio). Each

UNCORRECTED PROOF

tube was placed in the fast prep homogenizer on a predetermined 1 min cycle to ensure complete homogenization. Forty μl of each homogenate was aliquoted to a fresh tube and 50 μl of MeOH plus 150 μl of Methanol-containing Internal standard (25 ng/ml Imipramine HCl) was added. Each sample was mixed on a Bioshake for 1 min and then transferred to the freezer at −20 °C for at least 2 hours prior to the centrifugation at 2500 × g for 20 mins. The supernatants were then transferred to a 96-well plate for sampling by the LC–MS/MS. A Thermo TSQ Quantiva with Thermo Vanquish UHPLC system was used (Thermo Fisher Scientific Inc). Separation was achieved on a ACE-AR C18 (50 × 2.1 mm, 1.7 μm) column, with MilliQwater 0.1% formic acid (solvent A) and methanl-0.1% formic acid (solvent B) at 65 °C and at a flow rate of 0.8 ml/min. Positive ion spray voltage and vaporizer temperature were set at 3500 V and 450 °C respectively, while the ion transfer tube temperature was set at 365 °C. Finally, sheath gas and auxiliary gas pressures were fixed at 54 and 17 bar, respectively. Detection was performed using a multiple reaction monitoring (MRM) *via* a positive electrospray ionisation source spray voltage. Quantitative analysis was conducted by MRM at 229.00–246.00 m/z for PP2, 232.06–401.11 m/z for dasatinib and at 86.10–193.04 m/z for the internal standard Imipramine. Mass transitions were combined for each compound to maximise sensitivity.

2.3. in vitro studies

2.3.1. Cell viability and cytotoxicity assays

C2C12 mouse skeletal muscle myoblasts (Sigma-Aldrich) were cultured in Dulbecco's modified Eagle's medium (DMEM), containing 10% fetal bovine serum (Aurogene), 1% penicillin/streptomycin (Aurogene) and 1% L-glutamine (Aurogene) and maintained at 37 °C in 5% CO_2 – 95% air. After growing to 70% confluence, C2C12 cells were used for specific experimental assays, as indicated in the text.

Cell viability was evaluated using the Cell Counting Kit-8 (CCK-8, 96992 Sigma Aldrich)3636]. C2C12 cells were seeded in 96-well cultures at a density of approximately 4–4.5 × 10^3 cells *per* well. Sixteen hours after seeding, cells were treated with one of the test compounds, solubilized in DMSO (<0.15%) and dissolved in DMEM, at different concentrations: PP2 from 0.1 μM up to 300 μM and dasatinib from 0.1 μM up to 150 μM. Five hours following the exposure, 10 μl of CCK-8 were added into each well and then the plate was incubated for an additional 2 hours. The optical density of each well was determined using a microplate reader set to 450 nm (Victor Victor V31420-40, PerkinElmer, Wellesley, Massachusetts). Cell viability was expressed in percentage, according to the following formula: cell viability (%) = [(test value-blank) / (control value-blank) × 100], where the blank value represents that of a cell-free wells and the control value represents that of wells of cells treated with the vehicle alone (0.15% DMSO, for the highest concentration tested). The potential protective effect against hydrogen H_2O_2 (Sigma-Aldrich) cytotoxicity was evaluated pre-incubating the cells, with PP2 or dasatinib, 2 hours before the application of H_2O_2 (300 μM or 1 mM). Then, C2C12 cells were exposed to the same condition described above for the cells treated with the test compounds alone. The potential cytoprotective effect against H_2O_2-induced cytotoxicity was expressed according to the following formula: cell viability (%) = [(test value - blank) / (control value - blank) × 100], where the blank value represents that of a cell-free wells, the test value represents that of wells of cells treated with either one of the test compounds or H_2O_2 (300 μM or 1 mM) and the control value represents that of wells of cells treated with H_2O_2 alone (300 μM or 1 mM).

2.4. Statistics

All data are expressed as mean ± standard error of the mean (SEM). Multiple statistical comparisons between groups were performed by one-way ANOVA, with Bonferroni's *t*-test post hoc correction, when the null hypothesis was rejected ($p < 0.05$), to provide a better evaluation of intra- and intergroup variability and avoid false positives. If necessary, statistical analysis for direct comparison between two means was performed by unpaired Student's *t*-test The recovery score by the drug treatment, as percentage of change toward the WT value, has been evaluated according to the Standard Operating Procedures described in the Treat-NMD web site (http://www.treat-nmd.eu/research/preclinical/DMDSOPs), using the following equation:

Recovery score = [(*mdx* treated - *mdx* untreated) / (WT - *mdx* untreated)] × 100

3. Results and discussion

3.1. In vivo results

3.1.1. Effect of 5-week treatment with PP2 and dasatinib on body weight, forelimb strength, fatigue and torque

Drug treatments did not modify mice normal growth: an age-dependent increase in BW was observed in all groups during the experimental time window, with a BW value higher in *mdx* (either treated or not) *versus* WT at T4 and T5 (Fig. 1A). No abnormal gross findings were observed in animal well-being and no deaths were observed during the study period. As expected, an age-dependent increase of *in vivo* forelimb strength by grip test was observed, with *mdx* mice having always lower values than WT. To avoid any bias due to individual differences in BW, all forelimb strength values were normalized to BW. In PP2 treated *mdx* mice group, a significant increment in forelimb force was observed at T2 and T5, with a recovery score of about 43% and 29%, respectively. However, no significant effect was observed on this functional parameter in dasatinib-treated *mdx* mice (Fig. 1B). Another index of neuromuscular function is resistance to treadmill running until exhaustion, a composite measure of fatigability resembling the 6-minute walk test, used clinically for DMD patients. The test was performed at the beginning (T0) and at the end of the treatments (T5). At T5, the *mdx* mice groups maintained a lower running performance, *e.g.* reduced distance run, with respect to WT mice, even though in PP2 treated *mdx* mice a recovery score of about 56% was observed (data not shown). Furthermore, torque at T5 in anaesthetized mice was measured.*Mdx* mice, either treated or not, were significantly weaker than WT ones and no effect was observed on this parameter in *mdx* mice treated with either PP2 or dasatinib (Fig. 1C).

3.2. Ex vivo results

3.2.1. Effect of 5-week treatment with PP2 and dasatinib on both β-DG protein level and gene expression profile

In light of the poor efficacy on *in vivo* functional parameters, at the end of the treatments, we assessed the ability of both PP2 and dasatinib to modulate the expression of β-DG and its phosphorylated form in skeletal muscle (Fig. 2A). Accordingly, we assessed the β-DG signaling by measuring the ratio between β-DG and β-ACT (Fig. 2B) and the ratio between p-βDG and β-DG (Fig. 2C) in treated TA muscles. Interestingly, the treatments led to a significant increase in β-DG protein level and to a significant decrease of p-βDG/β-DG ratio in *mdx*-treated GC muscles with respect to vehicle-treated counterpart, corroborating the effect of both compounds. The effect was greater than that observed with the gold standard PDN, which maintained the same efficacy previously found [32]. We also performed real-time PCR experiments on GC muscles of WT and *mdx* mice, treated or not with PP2 or dasatinib, to assess the expression of key genes, such as β-DG and Utrn, as well as of PGC-1α, known to be involved in mechanical-metabolic coupling. We also investigated genes involved in autophagy (Bnip3), in

UNCORRECTED PROOF

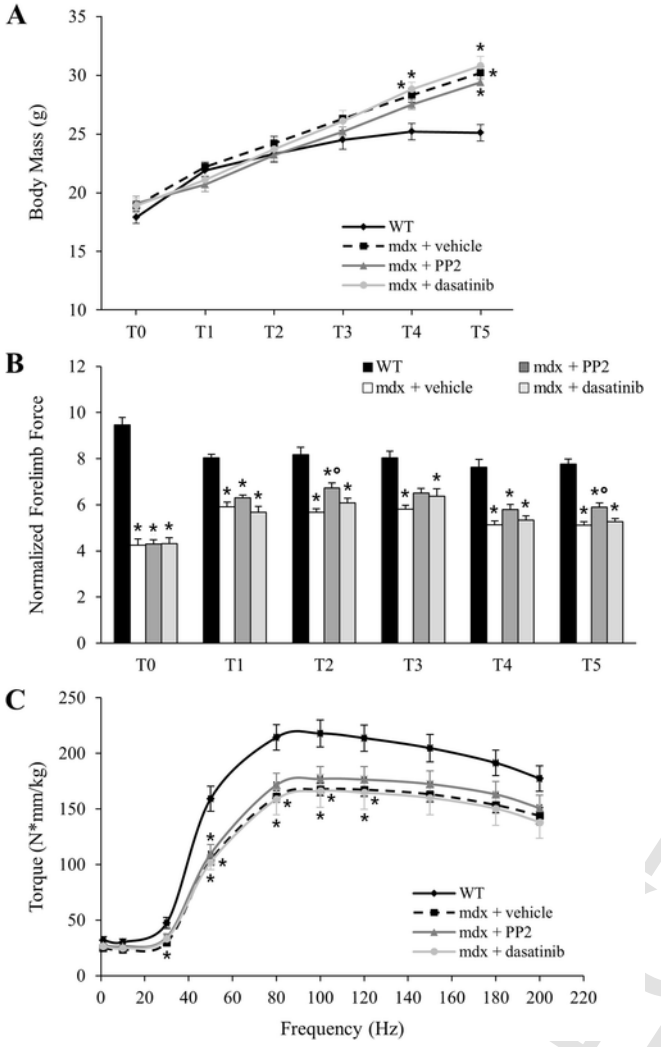

Fig. 1. Effect of 5-week treatment with PP2 and dasatinib on *in vivo* functional parameters. The figure shows: the variations in BW (A); forelimb maximal force normalized to BW (B) at the beginning (T0) and after 1 (T1), 2 (T2), 3 (T3), 4 (T4) and 5 (T5) weeks of treadmill-exercise protocol; isometric tetanic torque values of plantarflexor muscle normalized with respect to mouse BW (C) after 5 (T5) weeks of treadmill-exercise protocol for *mdx* mice both treated or not with one of the test compounds compared with a group of age-matched sedentary WT mice, monitored at the same time points of *mdx* counterparts. All values are mean ± S.E.M. from 6 to 8 mice for each group. A significant difference among groups was found by ANOVA analysis for A ($F > 7$; $4 \times 10^{-6} < p < 0.002$ for values at T4 and T5), B ($F > 12$; $1 \times 10^{-13} < p < 4 \times 10^{-5}$ for values from T0 to T5) and C ($F > 4$; $8 \times 10^{-5} < p < 0.02$ for values from 30 Hz to 120 Hz). Bonferroni post hoc corrections for individual differences between groups are as follows: significantly different with respect to * sedentary WT mice ($2 \times 10^{-13} < p < 0.008$), ° exercised *mdx* mice treated with vehicle ($0.002 < p < 0.003$).

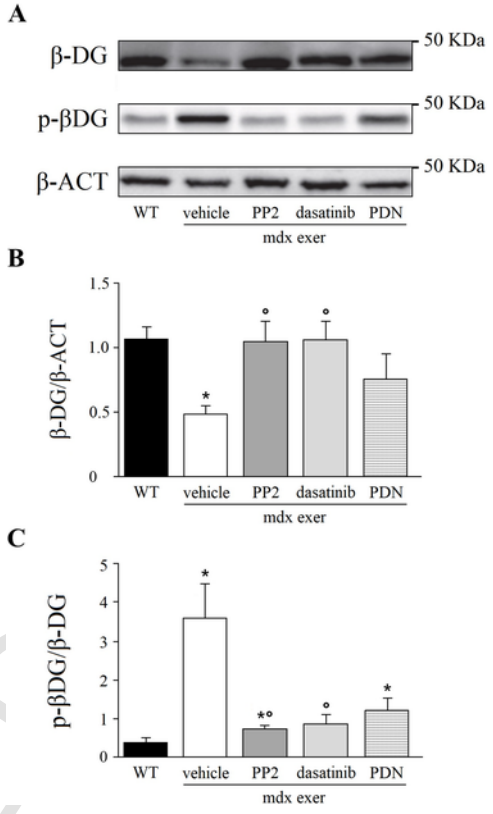

Fig. 2. Effect of 5-week treatment with PP2 and dasatinib on ratio of p-βDG/β-DG in TA muscles of both WT and *mdx* mice. The figure shows: representative western blots of the total β-DG, p-βDG and β-ACT (A); the ratio β-DG/β-ACT (B) and p-βDG/β-DG (C), in TA muscle from sedentary WT and exercised *mdx* mice, both treated or not with one of the test compounds. Each bar is the means ± S.E.M. of 4–5 mice *per* group. A significant difference among groups was found by unpaired Student's *t*-test analysis as follows: significantly different with respect to * exercised WT mice ($0.001 < p < 0.03$); ° exercised *mdx* mice treated with vehicle ($0.008 < p < 0.01$).

muscle fibrosis (TGF-β1), inflammation and oxidative stress (NOX) as well as Src-TK itself. Interestingly, gene expression profile of β-DG remains unchanged, indicating that both PP2 and dasatinib act at post-translational level. No significant differences were observed in gene expression of Utrn, Bnip3, TGF-β1, NOX and Src-TK of *mdx* treated mice with respect to the untreated counterpart, indicating that the treatments did not have an impact at transcriptional level of autophagy, inflammation and oxidative stress (Fig. S1).

3.2.2. Effect of 5-week treatment with PP2 and dasatinib on muscle histology

GC muscles clearly showed the typical dystrophic features, such as the alteration of muscle architecture, with the presence of necrotic areas, inflammatory infiltrates and non-muscle areas, likely due to deposition of fibrotic and adipose tissue. The presence of CNF, index of cyclic degeneration-regeneration events, was also clearly detectable (Fig. 3A). However, a great variability within different mice and within different fields of the same muscle was observed, which required a detailed morphometric analysis of large muscle sections to assess possible differences between groups. A reduction of the total area of damage was observed in GC muscle of *mdx* mice treated with both PP2 or dasatinib, without reaching statistical significance, likely due to the high variability between samples (Fig. 3B). A significant increase in the number of normal myocytes (NF), with peripheral nuclei, was observed in GC muscles treated with PP2, accompanied by a not significant 12% decrease in number of CNF, suggesting the ability of the drug to prevent the frequent degeneration/regeneration cycles, typical of dystrophic myofibers. In dasatinib-treated muscles, a similar trend of increase of normal myocytes was observed (Fig. 3C).

3.2.3. Effect of 5-week treatment on β-DG labelling in GC muscle

The observed rescue in expression of β-DG observed by western blot, lead us to perform immunofluorescence analysis in GC muscles to assess the possible effects of the treatment in rescuing β-DG levels in membrane. As expected, no detection of β-DG was found in untreated GC muscles membrane, while the presence of external laminin could be appreciated. In muscles treated with either dasatinib or PP2, only a faint staining was occasionally found in very restricted areas. These results, although promising, suggest that either the intensity or the duration of the treatments was not enough to lead to a detectable rescuing

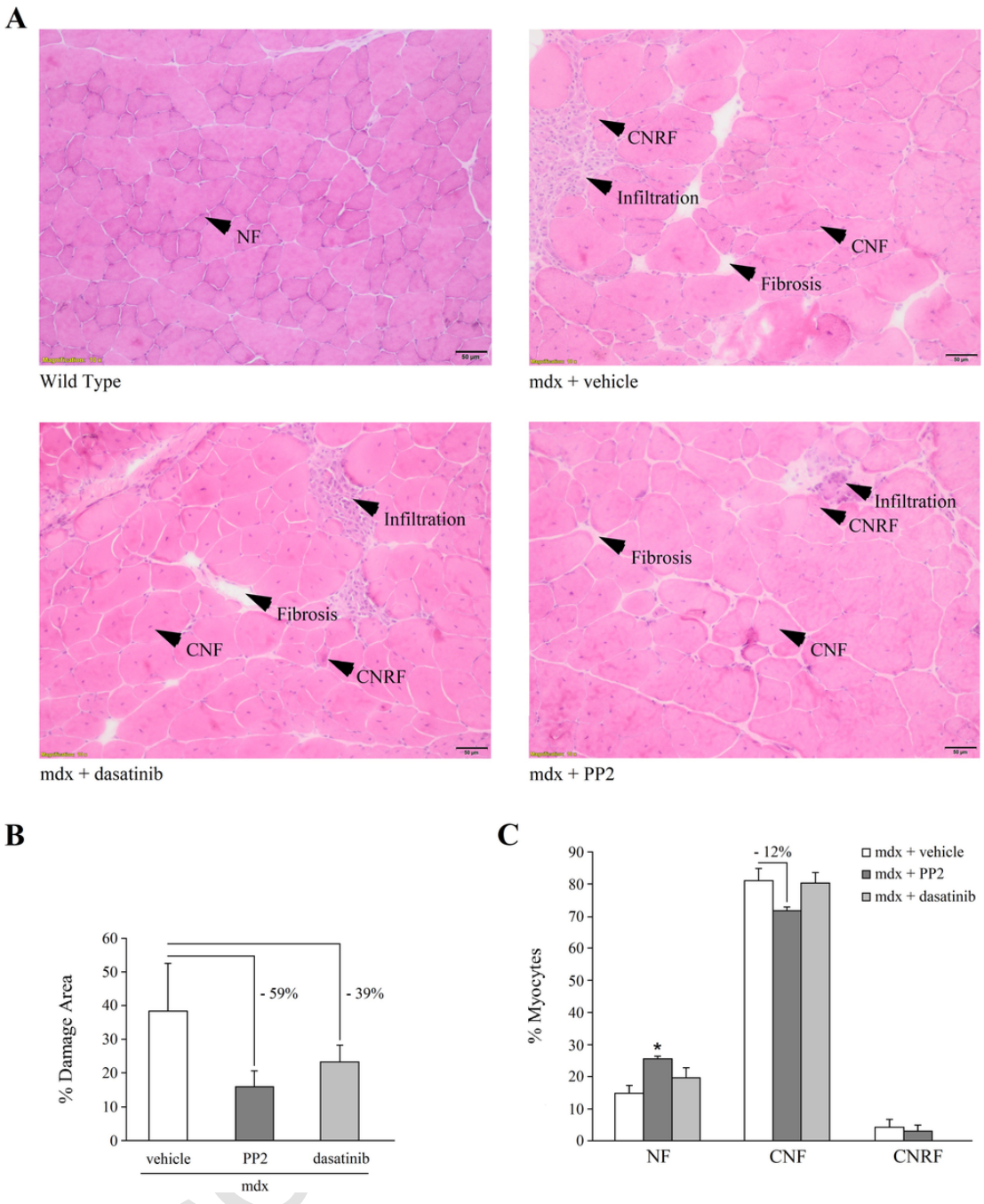

Fig. 3. Effect of 5-week treatment with PP2 and dasatinib on GC histology. (A) Samples of H&E staining showing the morphological profiles of GC muscles from WT mice (upper left panel), exercised *mdx* mice either treated (lower panel) or not (upper right panel) with one of the test compounds. The section from WT mice showed the typical structure of normal muscle fibres (NF), with peripheral nuclei, while exercised *mdx* treated or not with one of the test compounds clearly showed the poorly homogeneous structure typical of dystrophic muscle, with great variability in fibre dimension, centronucleated fibres (CNF), large areas of necrosis accompanied by mononuclear infiltrates and/or small centronucleated regenerating fibres (CNRF) and areas of non-muscle tissue, indicated by the arrows in the figure. The images are at 10X magnification. (B) The histograms show the percentage of the total damaged area of GC muscle of exercised *mdx* mice either treated or not with one of the test compounds. Each bar is the mean of at least 4 muscles and 3–4 fields *per* muscle. No statistical significance was found by ANOVA analysis, although a reduction of total damage area of 59% and 39% (indicated next to the line) for exercised *mdx* treated with PP2 and dasatinib respectively was observed. (C) The histograms show the percentage of NF, of CNF and CNRF of exercised *mdx* mice either treated or not with PP2 or dasatinib. Each bar is the mean of at least 4 muscles and 6 fields *per* muscle. A significant difference among groups was found by unpaired Student's *t*-test analysis as follows: * significantly different with respect to exercised *mdx* mice treated with vehicle ($p < 0.006$). No difference was observed in PP2-treated animals, although there was a 12% reduction in CNF (indicated above the line).

of the β-DG at sarcolemmal level, also in relation to protein turnover (Fig. 4).

3.2.4. *Effect of 5-week treatment with PP2 and dasatinib on muscle contraction parameters*

The effects of the treatments were evaluated on EDL muscle, a dystrophy-susceptible fast-twitch hind limb muscle. As expected, EDL muscles of untreated *mdx* mice had significantly lower values of specific twitch and tetanic force with respect to WT ones. No significant effect of the treatments was observed on either twitch (sPtw) or tetanic (sP0) force of EDL muscle, although a recovery score of about 57% was found on sPtw of PP2 treated *mdx* mice (Fig. 5A, B). In addition, the analysis of calcium-dependent parameters (ratio sPtw/sP0) indicated no effect of test compounds (data not shown). Furthermore, no signifi-

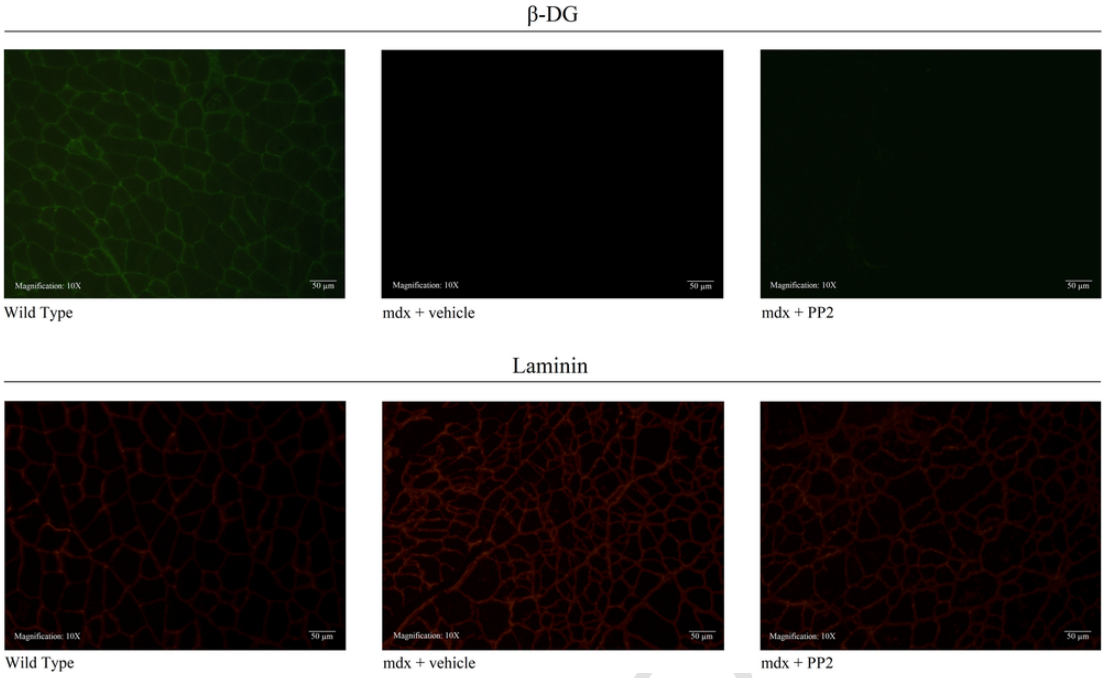

Fig. 4. Effect of 5-week treatment on β-DG labelling on GC muscle. Immunofluorescence staining for β-DG in GC muscles from WT mice, exercised *mdx* mice either treated or not with PP2 showed a faint effect not related to the treatment (upper panel). Dasatinib-treated muscle didn't show any appreciable β-DG expression. The sections were also stained for laminin as positive control (lower panel). The images are at 10X magnification.

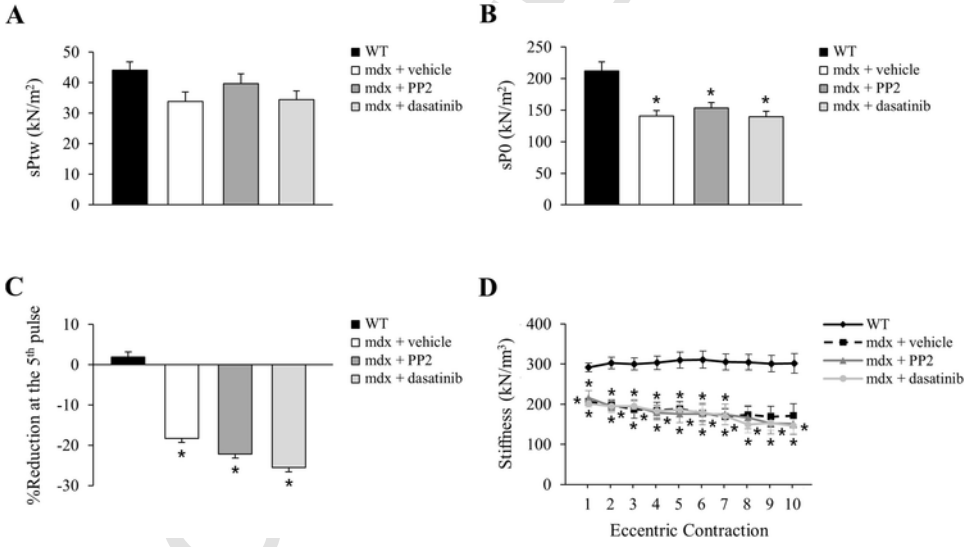

Fig. 5. Effect of 5-week treatment with PP2 and dasatinib on isometric contractile parameters of EDL muscle of WT and *mdx* mice. (A) The histograms show the normalized values of sPtw (measured in kN/m^2). All values are mean ± S.E.M. from 5 to 8 mice for each group. No significant difference among groups was found by ANOVA analysis. (B) The histograms show the normalized values of sP0 (measured in kN/m^2). All values are mean ± S.E.M. from 5 to 8 mice for each group. (C) The histograms show the reduction of tensions calculated at the 5^{th} pulse and is the mean ± S.E.M. for 5–11 mice *per* group. (D) The figure shows the stiffness (measured in kN/m^3) and is the mean ± S.E.M. for 5–7 mice *per* group. In B, C and D, a significant difference among groups was found by ANOVA analysis ($F > 4$; $p < 0.03$). Bonferroni post hoc correction for individual differences between groups is as follows: * significantly different with respect to sedentary WT mice ($5 \times 10^{-5} < p < 0.009$).

cant protection of both PP2 and dasatinib was observed either on eccentric contraction force drop calculated at the 5^{th} pulse (Fig. 5C) or on recovery from it (data not shown). Another parameter that can discriminate between WT and *mdx* muscles is stiffness. The *mdx* EDL muscles were less compliant to stretch with respect to WT ones, as shown by the lower value obtained by calculating the difference of force before and after the stretch. No amelioration of stiffness was observed with both treatments (Fig. 5D). In order to assess any potential direct effects of Src-TK inhibitors on muscle force, the effect of high concentrations of dasatinib was evaluated on sPtw and sP0 of EDL muscle *in vitro* (Fig. 6A, B). As it can be seen, both sPtw and sP0 underwent a comparable time-dependent decrease either in WT or in *mdx* EDL muscle; interestingly dasatinib showed a clear ability to further decrease both parameters in a concentration dependent manner, with respect to time-matched vehicle exposed muscles, with a slightly greater effect in *mdx versus* WT (Fig. 6A and B).

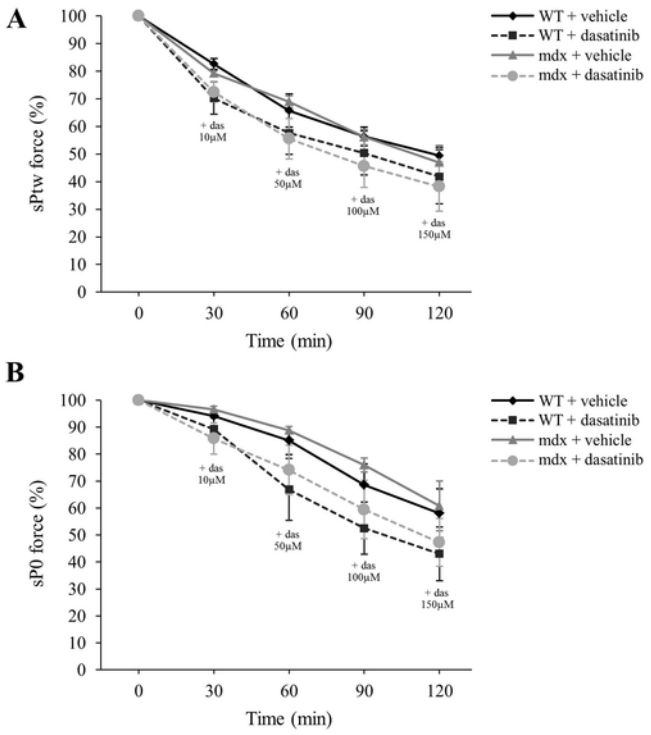

Fig. 6. EDL muscle contraction experiments with dasatinib *in vitro*. The figure shows the decrease of sPtw (A) and sP0 (B) force values of EDL muscles from WT and *mdx* mice, in presence of increasing *in vitro* concentrations of dasatinib (10, 50, 100, 150 μM) or of vehicle alone (DMSO 0.15% in Ringer's solution) over time (from 0 to 120 mins, with an interval of 30 mins between registration protocols). Each value is expressed as the percentage of reduction with respect to time point 0, taken as 100%. No statistically significant differences among groups were found by ANOVA analysis.

3.2.5. Effect of 5-week treatment with PP2 and dasatinib on vital organ mass

At necropsy, no significant differences were found in the normalized weight of vital organs (liver, kidney, heart and spleen), suggesting no gross toxic effects due to the treatments [37] (Fig. S2). Similarly, no significant differences were found in the normalized weight of EDL muscle between the experimental groups (data not shown).

3.2.6. Effect of 5-week treatment with PP2 and dasatinib on plasma biomarkers

CK, LDH and MMP-9. No significant amelioration was observed on either CK or LDH, biomarkers of sarcolemma fragility and metabolic sufferance, respectively, for both treatments. However, in dasatinib-treated *mdx* mice a 26% and 28% recovery score were observed for CK and LDH respectively. The plasmatic level of MMP-9, a zinc-metalloproteinase involved in degradation of extracellular matrix, is considered a biomarker of dystrophic pathology [38]. On this biomarker, a percent reduction of about 40% was observed in PP2-treated *mdx* mice, while no amelioration was observed for dasatinib-treated ones (Fig. 7).

3.2.7. Pharmacokinetic analysis of PP2 and dasatinib plasma and tissues levels

HPLC analyses were carried out to evaluate the traceability of PP2 and dasatinib in plasma and tissues (quadriceps and liver) of treated *mdx* mice. Dasatinib was not detectable in plasma, while PP2 was appreciable in a micromolar range (122.5–490 μM). Appreciable drugs' levels were found in quadriceps and livers of treated animals (Fig. 8). These results are in line with the finding that dasatinib is rapidly distributed in tissues [39]. Also, the level reached in skeletal muscle allows the biochemical action of PP2 and dasatinib to take place, considering that the inhibition of Src-TK occurs in a nanomolar range [40].

3.3. In vitro results

3.3.1. Evaluation of Src-TK inhibitors on cell viability and cytoprotective effect in C2C12 cells

A possible hypothesis for the limited efficacy of *in vivo* treatments is a muscle-specific cellular toxicity of both PP2 and dasatinib, that may impact the myogenic program of satellite cells involved in first steps of the regenerative process. Therefore, the effects of these two compounds on viability of undifferentiated C2C12 cells, a murine muscle derived satellite cell line, was evaluated both in normal growth conditions and in presence of H_2O_2-induced oxidative stress. Increasing concentrations of PP2 (0.1–300 μM) and dasatinib (0.1–150 μM) were tested on C2C12 to evaluate the potential cytotoxic drug action. PP2 exerted a mild (20%) but significant cytotoxic effect from the concentration of 3 μM onward, with no remarkable concentration-dependent action, while no effects were observed at lower concentrations (Fig. 9A). By contrast, dasatinib exerted a clear concentration-dependent effect, with a decrease of cell viability of more than 90% at the highest concentration tested. However, lower concentrations of dasatinib (0.1–1 μM) did not greatly modify C2C12 viability (Fig. 9B). To clarify the link between oxidative stress and satellite cell function, we tested the effect of increasing concentrations of H_2O_2 (10 μM-1 mM) on C2C12 cell viability. The exposure to H_2O_2 for 6 hours caused a decrease in the number of cells in a concentration-dependent manner (Fig. 9C). Considering that Src-TK is activated by oxidative stress, we evaluated the potential cytoprotective effects of PP2 and dasatinib by testing two cytotoxic concentrations of H_2O_2 (300 μM and 1 mM) on C2C12 cells, exposed to different concentrations of PP2 and dasatinib prior to the incubation with H_2O_2. The potential cytoprotection of PP2 0.1–100 μM and dasatinib 0.1–1 μM was tested, considering the limited direct toxicity of both compounds in the concentration range. The cytotoxic effect of 300 μM

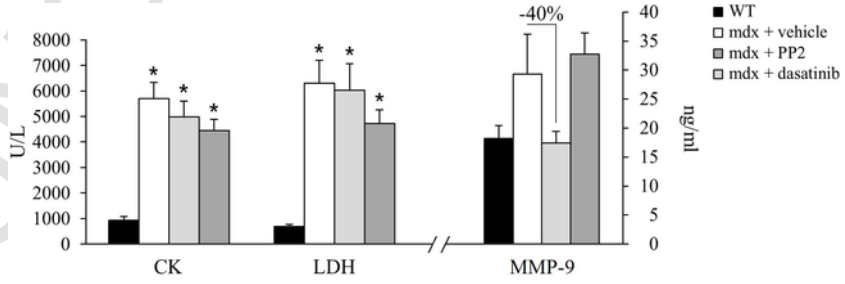

Fig. 7. Effect of 5-week treatment with PP2 and dasatinib on plasma biomarkers. The histograms show the plasma levels of CK, LDH and MMP-9 of sedentary WT and exercised *mdx* mice either treated or not with one of the test compounds. Each bar is the mean ± S.E.M. for 6–8 mice *per* group. For CK and LDH significant difference among groups was found by ANOVA analysis ($F > 9$; $1 \times 10^{-5} < p < 0.0002$). Bonferroni post hoc corrections for individual differences between groups is as follows: * significantly different with respect to sedentary WT mice ($2 \times 10^{-6} < p < 0.002$). For MMP-9, no significant difference among groups was found by ANOVA analysis, although a 40% reduction (indicated above the line) in MMP-9 plasma level of PP2 treated mice was observed .

UNCORRECTED PROOF

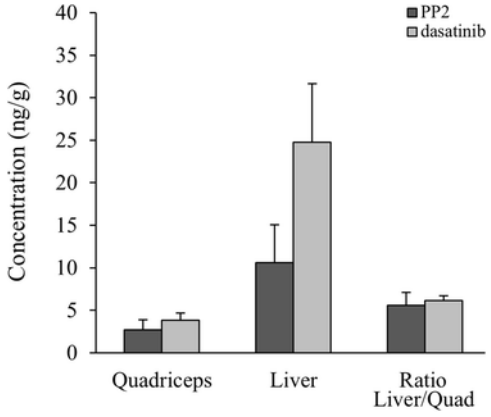

Fig. 8. PK analysis of PP2 and dasatinib in quadriceps and liver of treated mice. The histograms show the concentration (ng/g) of PP2 and dasatinib in quadriceps and liver of treated animals and the ratio between this latter and the quadriceps. All values are mean ± S.E.M. from 7- to 8 mice for each group. No significant difference among groups was found by Student *t*-test analysis.

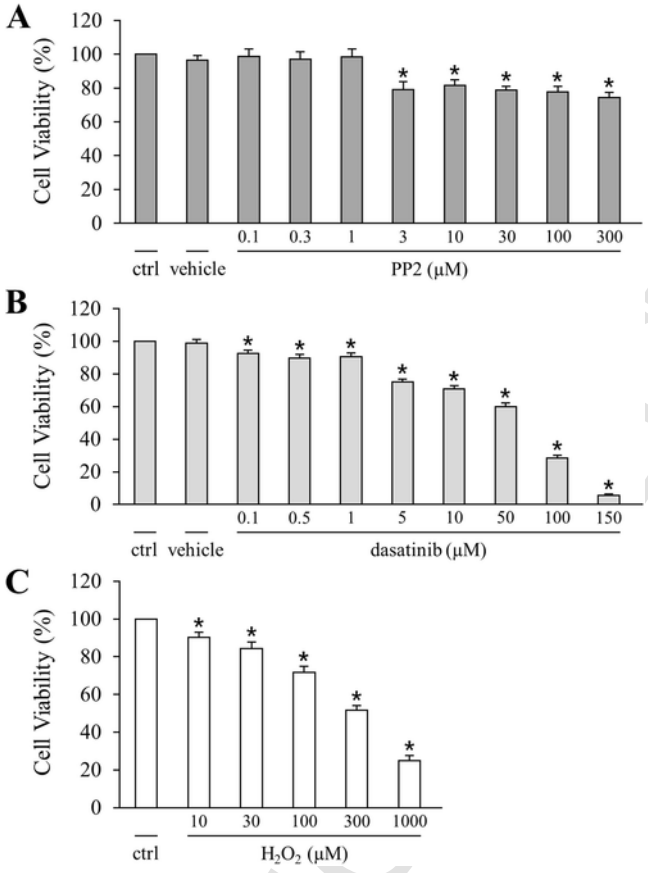

Fig. 9. Cytotoxic effect of PP2 and dasatinib. The figure shows the cytotoxic effect of increasing concentration of PP2 (A), dasatinib (B) and H_2O_2 (C) on cell viability. The results are expressed as the percentage of the control and presented as the mean ± SEM. Each data is from at least 12–48 replicates (wells) and 3–9 different culture dishes. The statistical significance between groups was evaluated by Student's *t*-test as follow: * significantly different with respect to the control value ($0.001 < p < 0.01$).

H_2O_2 was significantly counteracted by 0.3–100 μM PP2 (Fig. 10A) and, exclusively and to a lesser extent, by 0.1 μM dasatinib (Fig. 10B). Higher concentrations of dasatinib (0.5 μM and 1μM) were necessary to exert a cytoprotective effect against 1 mM H_2O_2 (Fig. 10B), whereas no significant protection was observed with PP2 (data not shown).

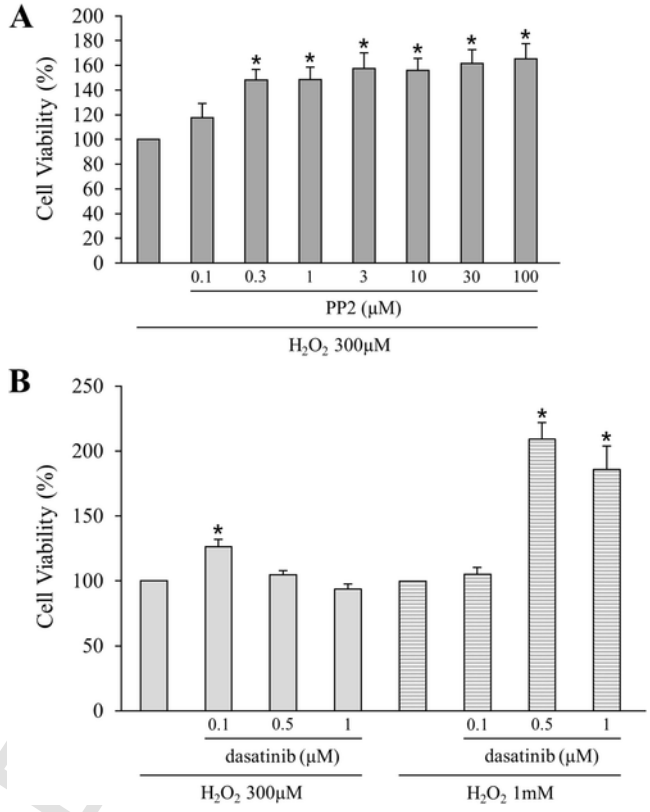

Fig. 10. Cytoprotective effect of PP2 and dasatinib. The figure shows the potential cytoprotective effect against H_2O_2-induced cytotoxicity of PP2 (D) and dasatinib (E), respectively. The results are expressed as the percentage of the control and presented as the mean ± SEM. Each data is from at least 19–20 replicates (wells) and 5 different culture dishes. The statistical significance between groups was evaluated by Student's *t*-test as follow: * significantly different with respect to the control value ($0.001 < p < 0.01$).

4. Conclusions

The complex cascade of events leading to muscle wasting in DMD is yet unclear and the complexity of the pathology pushes to search for drugs acting at upstream level of the pathological cascade, to exert a wider protection [3,25,41]. Increasing evidence suggest that the loss of dystroglycans fromsarcolemma of dystrophic muscle plays an important role in signaling alterations consequent to dystrophin absence. In particular, β-DG, through association with intracellular binding partners, works as a membrane stabilizer and is involved in signal transduction process that ensures adequate metabolic response to contractile stress [6,42]. In absence of dystrophin, β-DG is phosphorylated by a member of Src-TK family, leading to its internalization and degradation by proteasome [21]. This mechanism has been recently validated using the dystrophic *sapje* zebrafish [24]. The lower presence of β-DG at sarcolemma may be a crucial upstream event in the aberrant mechano-transduction occurring in dystrophic muscle. In fact, evidence in mechano-sensitive lung epithelial cells showed that β-DG modulates two independent pathways involved in mechano-transduction, *i.e.* extracellular signal regulated kinase 1/2 (ERK1/2) and AMPK, a well-known metabolic sensor. An alteration of this interaction, as occurring after silencing β-DG, leads to defective AMPK activation upon stretch and to excessive production of ROS [43,44]. A similar process may account for a basal deregulation of AMPK and the improper effects of exercise and drugs [9,31]. Due to the key role of β-DG to anchor cytolinkers, such as dystrophin or utrophin at the sarcolemma, we postulated that the inhibition of Src-TKs could be a feasible approach to preserve DGC and to control pathology progression.

We presently investigated the effect of two small molecules acting as Src-TK inhibitors: dasatinib, already approved as anticancer drug, and the more selective PP2, by means of 5-week treatment preclinical study in exercised *mdx* mouse model.

To investigate the upstream effect of the treatments, we validated our proof-of-concept study, by measuring β-DG protein levels by means of western blot analysis. Muscles of treated animals showed higher levels of β-DG, and the efficacy of PP2 and dasatinib in restoring physiological levels of β-DG was higher than that found with the gold standard PDN [32]. Thus, these first results in the rodent model confirmed the mechanism of action of Src-TKs inhibitors, as observed in the simpler model of *sapje* zebrafish [24]. Accordingly, as underlined by the HPLC results, both drugs reach skeletal muscle and likely accumulate herein at concentrations able to exert their main mechanism of action. Gene expression analysis showed that both compounds act mainly at post-translational level, preventing the phosphorylation and degradation of β-DG, since the expression of key markers of inflammation, autophagy and oxidative stress remained unchanged. In addition, the modulation of functional readout parameters by the two drugs was modest. While PP2 could improve forelimb force *in vivo*, no effect was observed on this parameter with dasatinib; similarly, neither drugs ameliorated fatigability to treadmill running. *Ex vivo*, no protection was observed on contraction parameters of EDL muscle of drug-treated animals. Interestingly, immunofluorescence analysis showed that the presence of β-DG at membrane was modest, if any. Then , although the main action of the drugs was confirmed, issues related to treatments dose or duration, did not allow to ensure a proper restoration of DGC in membrane, therefore to achieve a considerable improvement in muscle function; this, also in consideration of the concomitant lack of dystrophin that our treatments did not address. Importantly, the exposure level was however allowing a downstream effect of the treatments, mainly addressing inflammation and oxidative stress, since some of the results obtained are encouraging. Notably, the histological profile of GC treated muscles was improved, in term of reduction of total damaged area and in the increase of normal peripherally nucleated myofiber. This effect was more appreciable for PP2, and supports the hypothesis that the drug may positively impact on degeneration-regeneration cycles. At biochemical level, PP2 reduced plasmatic secretion of MMP-9, a biomarker of dystrophic pathology. This result is in line with the evidence suggesting that the inhibition of Src-TK suppresses the secretion of MMP-9 [45]. In parallel, dasatinib reduced both CK and LDH plasma levels. Although this latter effect did not reach a statistical significance, it helps to rule out the occurrence of a potential muscle-specific side effect in an overt myopathic conditions, a risk that has been reported in cancer patients [46,47].

The lack of efficacy on functional parameters, despite the restoration of physiological level of β-DG, opens various hypotheses. The first one, foresees the possibility that β-DG is not rescued at the membrane, as supported by immunofluorescence results, maybe in relation to the short duration of the treatment in a phase of active muscle pathology.

Another possible hypothesis for the lack of *in vivo* efficacy, is the occurrence of a muscle-specific cellular toxicity. Although the decrease in CK plasma levels would argue against this assumption [46,47], we cannot rule out a cytotoxic action of these two drugs, known to act as antitumoral compounds, in affecting the myogenic program of satellite cells involved in the first steps of regeneration, *i.e.* cell commitments and proliferation [48–50].

Our *in vitro* results, obtained in murine muscle derived satellite cell line C2C12, showed indeed that dasatinib, and to a lesser extent PP2, causes a concentration-dependent cytotoxicity. However, this effect was observed at relatively high concentrations, which likely exceeded those reached after *in vivo* exposure. Also, this was less relevant for PP2, suggesting that Src-TK is marginally involved in satellite cells viability and that this cytotoxic mechanism plays a minor role in the lack of *in vivo* effects. According to this view, the same cytotoxic concentrations of dasatinib induced only a slight decrease in contractile force when applied acutely *in vitro* to EDL muscle. Furthermore, PP2 and dasatinib were able instead to determine a protective effect against H_2O_2-induced cytotoxicity, although with a different potency, suggesting that the cytotoxic action of oxidative agents in satellite cells is in part mediated by activation of Src-TK. In this respect, both compounds should be able to exert a therapeutic effect in dystrophic muscle, considering the key role of unbalanced oxidative stress for pathology progression and impaired regeneration [14,30,51]

Our results then open interesting perspectives, as they are pilot positive data about the possibility to correct an upstream defects in dystrophic muscle (*i.e.* the loss of β-DG, by modulating Src-TK) with no overt signs of toxicity, although it remains to be elucidated the mechanism for minor efficacy on pathology-related parameters.

Taken together, all these observations push us to conduct further preclinical studies with dasatinib and PP2, in order to better comprehend the interest of this class of compounds for DMD treatment. In particular, we are currently working to obtain novel formulations that will allow the administration *via* oral route and consequently perform dose-response study over longer exposure time [52]. This would help to better assess the possibility to obtain a greater effect on β-DG level at sarcolemma and to exert a better control of muscle functionality *via* both upstream and downstream effects related to proper Src-TK inhibition. The potential efficacy of these small molecules are likely to synergistically act in concomitant administration with utrophin upregulators or exon skipping or genome editing approaches [3,41], in order to obtain a greater rescue of the DGC complex and a better control of pathology progression, another possibility that will be further investigated.

PP2 turned out to be more effective and less cytotoxic, pushing us to consider it as a lead compound for the design of Src-TK inhibitors useful for DMD treatment, based on *in silico* and *in vitro* approaches [51,53,54]. However, dasatinib has been recently approved by FDA for the treatment of chronic myeloid leukemia in pediatric patients, while pediatric trials are ongoing by EMA to approve the use of this drug. For these reasons, dasatinib could be more easily repurposed for DMD patients upon a further validation of its potential efficacy.

Competing interests

The research has been given ethical approval. No conflicts of interest, financial or otherwise, are declared by the author(s).

Part of the work was in the frame of an MSD fellowship of the Italian Pharmacological Society to the project “Searching for orphan drugs for the therapy of Duchenne Muscular Dystrophy: potential role of Src tyrosine kinase inhibitors” of Dr. Anna Cozzoli.

Authors contributions

ADL elaborated the hypothesis and designed the studies; PM, AC, RFC conducted drug treatment and *in vivo* and *ex vivo* physiology experiments and determination of plasma biomarkers; FS conducted *in vitro* studies on C2C12 cells; AG, MDB and OC performed histology experiments and analysis; AC and ND supervised and performed PK analysis in plasma samples; EC and GMC designed and conducted qPCR and Western blot experiment and analyzed the results; FS organized figures and statistical analysis and with AC wrote a manuscript draft; FS, OC, PM and ADL revised the manuscript; ADL and JFR supervised experiments and analysis and finalized manuscript writing. All authors approved the manuscript.

UNCORRECTED PROOF

Acknowledgements

This work has been supported by a grant to ADL from Dutch Duchenne Parent Project (NL DPP) 2015, entitled "Preclinical studies to validate cSrc tyrosine kinase as therapeutic target in Duchenne muscular dystrophy".

Appendix A. Supplementary data

Supplementary material related to this article can be found, in the online version, at doi:https://doi.org/10.1016/j.phrs.2019.104260.

References

[1] E.P. Hoffman, D. Dressman, Molecular pathophysiology and targeted therapeutics for muscular dystrophy, Trends Pharmacol. Sci. 22 (2001) 465–470.
[2] K. Bushby, et al., Diagnosis and management of Duchenne muscular dystrophy, part 1: diagnosis, and pharmacological and psychosocial management, Lancet Neurol. 9 (2010) 77–93.
[3] T. Koo, et al., Functional rescue of dystrophin deficiency in mice caused by frameshift mutations using campylobacter jejuni Cas9, Mol. Ther. J. Am. Soc. Gene Ther. 26 (2018) 1529–1538.
[4] A. Aartsma-Rus, et al., Theoretic applicability of antisense-mediated exon skipping for Duchenne muscular dystrophy mutations, Hum. Mutat. 30 (2009) 293–299.
[5] C. Pichavant, et al., Current status of pharmaceutical and genetic therapeutic approaches to treat DMD, Mol. Ther. J. Am. Soc. Gene Ther. 19 (2011) 830–840.
[6] C.J. Moore, S.J. Winder, The inside and out of dystroglycan post-translational modification, Neuromuscul. Disord. NMD 22 (2012) 959–965.
[7] J.L. Ilsley, M. Sudol, S.J. Winder, The interaction of dystrophin with beta-dystroglycan is regulated by tyrosine phosphorylation, Cell. Signal. 13 (2001) 625–632.
[8] V. Ljubicic, et al., Chronic AMPK activation evokes the slow, oxidative myogenic program and triggers beneficial adaptations in mdx mouse skeletal muscle, Hum. Mol. Genet. 20 (2011) 3478–3493.
[9] P. Mantuano, et al., Effect of a long-term treatment with metformin in dystrophic mdx mice: A reconsideration of its potential clinical interest in Duchenne muscular dystrophy, Biochem. Pharmacol. 154 (2018) 89–103.
[10] F. Sotgia, et al., Localization of phospho-beta-dystroglycan (pY892) to an intracellular vesicular compartment in cultured cells and skeletal muscle fibers in vivo, Biochemistry 42 (2003) 7110–7123.
[11] R. Pal, et al., Src-dependent impairment of autophagy by oxidative stress in a mouse model of Duchenne muscular dystrophy, Nat. Commun. 5 (2014) 4425.
[12] G.M. Camerino, et al., Gene expression in mdx mouse muscle in relation to age and exercise: aberrant mechanical-metabolic coupling and implications for pre-clinical studies in Duchenne muscular dystrophy, Hum. Mol. Genet. 23 (2014) 5720–5732.
[13] O.L. Gervásio, N.P. Whitehead, E.W. Yeung, W.D. Phillips, D.G. Allen, TRPC1 binds to caveolin-3 and is regulated by Src kinase - role in Duchenne muscular dystrophy, J. Cell. Sci. 121 (2008) 2246–2255.
[14] R. Burdi, et al., Multiple pathological events in exercised dystrophic mdx mice are targeted by pentoxifylline: outcome of a large array of in vivo and ex vivo tests, J. Appl. Physiol. Bethesda Md 1985 106 (2009) 1311–1324.
[15] T.A. Rando, Oxidative stress and the pathogenesis of muscular dystrophies, Am. J. Phys. Med. Rehabil. 81 (2002) S175–S186.
[16] T. Gamberi, et al., Proteome analysis in dystrophic mdx mouse muscle reveals a drastic alteration of key metabolic and contractile proteins after chronic exercise and the potential modulation by anti-oxidant compounds, J. Proteomics 170 (2018) 43–58.
[17] R. Paletta-Silva, N. Rocco-Machado, J.R. Meyer-Fernandes, NADPH oxidase biology and the regulation of tyrosine kinase receptor signaling and cancer drug cytotoxicity, Int. J. Mol. Sci. 14 (2013) 3683–3704.
[18] E. Giannoni, M.L. Taddei, P. Chiarugi, Src redox regulation: again in the front line, Free Radic. Biol. Med. 49 (2010) 516–527.
[19] G. Miller, et al., Preventing phosphorylation of dystroglycan ameliorates the dystrophic phenotype in mdx mouse, Hum. Mol. Genet. 21 (2012) 4508–4520.
[20] E. Gazzerro, et al., Therapeutic potential of proteasome inhibition in Duchenne and Becker muscular dystrophies, Am. J. Pathol. 176 (2010) 1863–1877.
[21] S. Assereto, et al., Pharmacological rescue of the dystrophin-glycoprotein complex in Duchenne and Becker skeletal muscle explants by proteasome inhibitor treatment, Am. J. Physiol. Cell. Physiol. 290 (2006) C577–C582.
[22] P. Grumati, et al., Autophagy is defective in collagen VI muscular dystrophies, and its reactivation rescues myofiber degeneration, Nat. Med. 16 (2010) 1313–1320.
[23] R. Roskoski, Src protein-tyrosine kinase structure, mechanism, and small molecule inhibitors, Pharmacol. Res. 94 (2015) 9–25.
[24] L. Lipscomb, R.W. Piggott, T. Emmerson, S.J. Winder, Dasatinib as a treatment for Duchenne muscular dystrophy, Hum. Mol. Genet. 25 (2016) 266–274.
[25] A. De Luca, et al., Gentamicin treatment in exercised mdx mice: identification of dystrophin-sensitive pathways and evaluation of efficacy in work-loaded dystrophic muscle, Neurobiol. Dis. 32 (2008) 243–253.
[26] A. De Luca, et al., A multidisciplinary evaluation of the effectiveness of cyclosporine a in dystrophic mdx mice, Am. J. Pathol. 166 (2005) 477–489.
[27] T. O'Hare, et al., In vitro activity of Bcr-Abl inhibitors AMN107 and BMS-354825 against clinically relevant imatinib-resistant Abl kinase domain mutants, Cancer Res. 65 (2005) 4500–4505.
[28] K. Taniguchi, et al., Inhibition of Src kinase blocks high glucose-induced EGFR transactivation and collagen synthesis in mesangial cells and prevents diabetic nephropathy in mice, Diabetes 62 (2013) 3874–3886.
[29] R.F. Capogrosso, et al., Ryanodine channel complex stabilizer compound S48168/ARM210 as a disease modifier in dystrophin-deficient mdx mice: proof-of-concept study and independent validation of efficacy, FASEB J. Off. Publ. Fed. Am. Soc. Exp. Biol. 32 (2018) 1025–1043.
[30] R.F. Capogrosso, et al., Assessment of resveratrol, apocynin and taurine on mechanical-metabolic uncoupling and oxidative stress in a mouse model of duchenne muscular dystrophy: A comparison with the gold standard, α-methyl prednisolone, Pharmacol. Res. 106 (2016) 101–113.
[31] R.F. Capogrosso, et al., Contractile efficiency of dystrophic mdx mouse muscle: in vivo and ex vivo assessment of adaptation to exercise of functional end points, J. Appl. Physiol. Bethesda Md 1985 122 (2017) 828–843.
[32] R. Tamma, et al., Effects of prednisolone on the dystrophin-associated proteins in the blood-brain barrier and skeletal muscle of dystrophic mdx mice, Lab. Investig. J. Tech. Methods Pathol. 93 (2013) 592–610.
[33] G.M. Camerino, et al., Effects of nandrolone in the counteraction of skeletal muscle atrophy in a mouse model of muscle disuse: molecular biology and functional evaluation, PloS One 10 (2015), e0129686.
[34] S.A. Bustin, et al., The MIQE guidelines: minimum information for publication of quantitative real-time PCR experiments, Clin. Chem. 55 (2009) 611–622.
[35] R.W. Grange, T.G. Gainer, K.M. Marschner, R.J. Talmadge, J.T. Stull, Fast-twitch skeletal muscles of dystrophic mouse pups are resistant to injury from acute mechanical stress, Am. J. Physiol. Cell Physiol. 283 (2002) C1090–1101.
[36] M.V. Berridge, P.M. Herst, A.S. Tan, Tetrazolium dyes as tools in cell biology: new insights into their cellular reduction, Biotechnol. Annu. Rev. 11 (2005) 127–152.
[37] Y. Piao, Y. Liu, X. Xie, Change trends of organ weight background data in sprague dawley rats at different ages, J. Toxicol. Pathol. 26 (2013) 29–34.
[38] V.D. Nadarajah, et al., Serum matrix metalloproteinase-9 (MMP-9) as a biomarker for monitoring disease progression in Duchenne muscular dystrophy (DMD), Neuromuscul. Disord. NMD 21 (2011) 569–578.
[39] D.R. Duckett, M.D. Cameron, Metabolism considerations for kinase inhibitors in cancer treatment, Expert Opin. Drug Metab. Toxicol. 6 (2010) 1175–1193.
[40] S. Rao, et al., Target modulation by a kinase inhibitor engineered to induce a tandem blockade of the epidermal growth factor receptor (EGFR) and c-Src: the concept of type III combi-targeting, PloS One 10 (2015), e0117215.
[41] J.M. Tinsley, et al., Daily treatment with SMTC1100, a novel small molecule utrophin upregulator, dramatically reduces the dystrophic symptoms in the mdx mouse, PloS One 6 (2011), e19189.
[42] G.A. Rezniczek, et al., Plectin 1f scaffolding at the sarcolemma of dystrophic (mdx) muscle fibers through multiple interactions with beta-dystroglycan, J. Cell. Biol. 176 (2007) 965–977.
[43] D. Takawira, G.R.S. Budinger, S.B. Hopkinson, J.C.R. Jones, A dystroglycan/plectin scaffold mediates mechanical pathway bifurcation in lung epithelial cells, J. Biol. Chem. 286 (2011) 6301–6310.
[44] G.R.S. Budinger, et al., Stretch-induced activation of AMP kinase in the lung requires dystroglycan, Am. J. Respir. Cell Mol. Biol. 39 (2008) 666–672.
[45] P. Cortes-Reynosa, T. Robledo, M. Macias-Silva, S.V. Wu, E.P. Salazar, Src kinase regulates metalloproteinase-9 secretion induced by type IV collagen in MCF-7 human breast cancer cells, Matrix Biol. J. Int. Soc. Matrix Biol. 27 (2008) 220–231.
[46] N.I. AlJohani, S. Carette, J.H. Lipton, Inclusion body myositis in a patient with chronic myeloid leukemia treated with dasatinib: a case report, J. Med. Case Reports 9 (2015) 214.
[47] B. Uz, I. Dolasik, An unexpected and devastating adverse event of dasatinib: Rhabdomyolysis, Leuk. Res. Rep. 5 (2016) 1–2.
[48] S. Puvanenthiran, S. Essapen, A.M. Seddon, H. Modjtahedi, Impact of the putative cancer stem cell markers and growth factor receptor expression on the sensitivity of ovarian cancer cells to treatment with various forms of small molecule tyrosine kinase inhibitors and cytotoxic drugs, Int. J. Oncol. 49 (2016) 1825–1838.
[49] L. Porcelli, et al., Synergistic antiproliferative and antiangiogenic effects of EGFR and mTOR inhibitors, Curr. Pharm. Des. 19 (2013) 918–926.
[50] A. Curci, A. Mele, G.M. Camerino, M.M. Dinardo, D. Tricarico, The large conductance Ca(2+) -activated K(+) (BKCa) channel regulates cell proliferation in SH-SY5Y neuroblastoma cells by activating the staurosporine-sensitive protein kinases, Front. Physiol. 5 (2014) 476.
[51] M. De Bellis, et al., Dual action of mexiletine and its pyrroline derivatives as skeletal muscle sodium channel blockers and anti-oxidant compounds: toward novel therapeutic potential, Front. Pharmacol. 8 (2017) 907.
[52] A. Cutrignelli, et al., Dasatinib/HP-β-CD inclusion complex based aqueous formulation as a promising tool for the treatment of paediatric neuromuscular disorders, Int. J. Mol. Sci. 20 (2019).
[53] D. Tricarico, et al., Structural nucleotide analogs are potent activators/inhibitors of pancreatic β cell KATP channels: an emerging mechanism supporting their use as antidiabetic drugs, J. Pharmacol. Exp. Ther. 340 (2012) 266–276.
[54] S.J. Wacker, et al., Identification of selective inhibitors of the potassium channel Kv1.1-1.2((3)) by high-throughput virtual screening and automated patch clamp, ChemMedChem 7 (2012) 1775–1783.

UNCORRECTED PROOF